Acta Oceanol. Sin., 2024, Vol. 43, No. 2, P. 111–119
https://doi.org/10.1007/s13131-023-2195-5
http://www.aosocean.com
E-mail: ocean2@hyxb.org.cn

Geochemistry of volcanic glass from Mahanadi offshore region, eastern continental margin of India: Constraints on the contribution of latest Toba super-eruption

Muralidhar Kocherla[1]*, Durbar Ray[1], Manavalan Satyanarayanan[2], Hilda Joao[1], Virsen Gaikwad[1], P.B Ramamurty[2]

[1] CSIR-National Institute of Oceanography, Dona Paula 403004, Goa, India

[2] CSIR-National Geophysical Research Institute, Uppal Road, Hyderabad 500007, India

Received 17 November 2022; accepted 17 March 2023

Abstract

The tephra layers in multiple sediment cores from the offshore region of the Mahanadi basin in the northern Bay of Bengal were investigated for possible volcanic sources. The glass shards from those tephra layers were studied for size distribution, texture, and elemental geochemistry to establish chronostratigraphic markers for regional and global Quaternary correlation. The textural features of fine-grained (silty) volcanic glasses suggest the distal source of these tephra deposits. Major element composition with elevated SiO_2 contents ranging between 75%–76% and dominance of K_2O (> 4.5%) over CaO (< 0.9%) suggest ashes have originated from siliceous rhyolitic melts, similar to the petrographic composition of tephra from the Toba volcano. The bulk trace element compositions of the same glass shards were comparable with those reported in the youngest Toba tephra reported elsewhere. Likewise, the LREE-dominated chondrite normalized REE profiles of tephra from the Mahanadi basin closely resemble the characteristic REE patterns in Toba ash from other parts of the Indian Ocean and thus confirmed the contribution of the youngest Toba super-eruption for this ash layers.

Key words: Mahanadi basin, Bay of Bengal, volcanic glass, glass morphology, glass-chemistry.

Citation: Kocherla Muralidhar, Ray Durbar, Satyanarayanan Manavalan, Joao Hilda, Gaikwad Virsen, Ramamurty P.B. 2024. Geochemistry of volcanic glass from Mahanadi offshore region, eastern continental margin of India: Constraints on the contribution of latest Toba super-eruption. Acta Oceanologica Sinica, 43(2): 111–119, doi: 10.1007/s13131-023-2195-5

1 Introduction

Mahanadi is a major river in eastern India, flowing over the states of Chhattisgarh and Odisha. The offshore area of the lower course of this river basin off the Odisha coast is a pull-apart basin; it originated during the break-up of Gondwana land in late Jurassic time (Rao et al., 1997; Sastri et al., 1981; Subrahmanyam et al., 2008). This offshore basin is of typical continental type and is bounded by the 85°E Ridge in the west and by N-S trending fault in the east (Fuloria et al., 1992). An earlier study indicated that this continental basement is mostly made of metamorphic rocks, including Eastern Ghats Granulites, overlain by sediments of variable age groups of upper cretaceous to recent type (Fuloria et al., 1992).

The Toba supervolcano eruption at 74 ka was one of Earth's most significant known eruptions in the past 2.5 million years. The Toba supervolcano erupted about minimum of ~2 800 km^3 volume of magma, of which at least 800 km^3 was deposited in the form of ash fall. This volcanic ash may be completely of volcanic origin and dispersed world widely because of high drag coefficients on the predominantly bubble-wall shards. Volcanic glsss-shards of this shape are broken from the walls of spherical vesicles, which was formed in high prosperity in isotropic strain shadows near the phenocrysts in this crystal-rich magma (Rose and Chesner, 1987). The Youngest Toba Tuff (YTT) occurs across peninsular India and in the Indian Ocean (Ninkovich et al., 1978; Westgate et al., 1998). Deposits of the Youngest Toba Tuff (YTT) eruption are found northwest of the vent, over the Indian subcontinent and the Arabian Sea (Pattan et al., 1999, 2001), and to the east in the South China Sea (Bühring and Sarnthein, 2000; Song et al., 2000; Liang et al., 2001). Here we, for the first time, describe the occurrence of volcanic ash layers within subsurface sediment across this offshore basin. To address the nature of magma involved in the genesis of these volcanic ashes, the glass shards from those ash layers were thoroughly investigated for physical characteristics and elemental geochemistry. Usually, the identification of volcanic sources for such tephra layers is another essential aspect, as it may provide helpful information on different aspects of volcanic history (Kennet, 1981; Fisher and Schmincke, 1984) as well as regarding sediment stratigraphy. In the present study, the geochemical features of available glass shards were also compared with Toba tephra, which broadly dispersed over the vast area of the Indian Ocean (Dehn et al., 1991; Pattan, 2002; Pattan et al., 2010; Mascarenhas–Pereira et al., 2016; Amonkar et al., 2020) to ascertain the particular Toba events (i.e., young, middle and oldest); as the source for sedimentary ash layers in the Mahanadi basin.

2 Collection of samples and analytical methods

In May 2007, during a cruise (MD-161) onboard RV *Marion Dufresne* in the northern Bay of Bengal, 05 long sediment cores of the length of 25 m to 50 m were collected from the offshore region of the Mahanadi basin (Fig. 1). Those core sampling sites are

*Corresponding author, E-mail: kocherla@nio.org

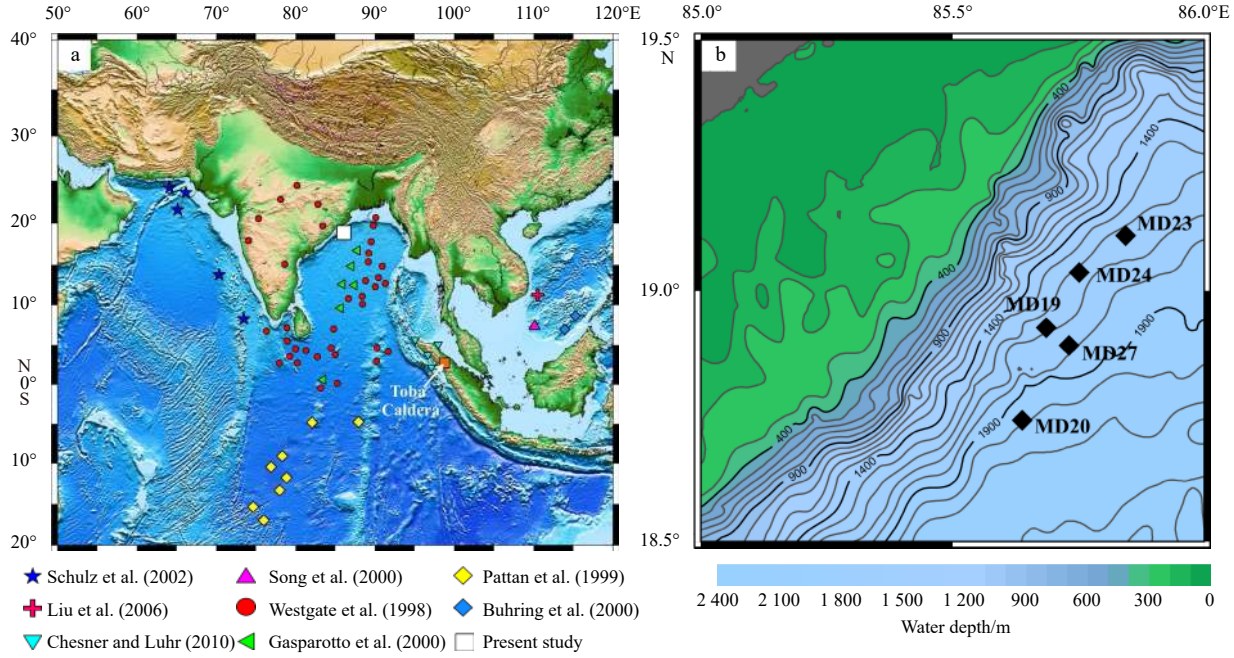

Fig. 1. Occurrences of the Youngest Toba Tuff (YTT) across the Indian Ocean region, southern Asia, and the South China Sea (modified from Lane et al., 2013; Westaway et al., 2011) (a). Bathymetric map of the study area in Mahanadi offshore region, east coast of India (b). Bathymetry data of the studied area was derived from GEBCO Compilation Group (2020) GEBCO 2020 Grid (doi: 10.5285/a29c5465-b138-234d-e053-6c86abc040b9).

mostly lying at the water depths of about 1 400 m to 2 000 m at the deeper part of the continental slope between 85.6°E and 85.85°E. The details of those sampling sites are mentioned in Table 1. Each core showed the presence of very distinct volcanic ash layers at the sediment depths between 09-22 mbsf. In the shore-based laboratory, those ash layers were carefully chopped out from the sediment cores and used for the present study. From those ash samples, the available volcanic glass shards were separated and analyzed for detailed texture, morphology, major, trace, and rare earth element compositions.

2.1 *Physical features of ash layers*

To investigate the particle size of the tephra, about 10 g of ash sample from each core was thoroughly cleaned and dried. The dry samples were treated with (1N) HCl to separate from carbonates and then thoroughly rinsed with Milli-Q water. Then the samples were sieved through multiple analytical sieves having pore sizes of 600 μm, 365 μm, 250 μm, 125 μm, and 63 μm, and thus, the weight percentages of each size fraction were estimated by using a microbalance. The volcanic glass shards available in each ash layer were examined with an X-ray diffractometer (Regaku Ultima IV) within the 2θ ranges between 10° to 57° to confirm their glassy nature. Several randomly selected glass particles of each ash layer were thoroughly examined for external morphologies with an optical microscope (Nikon's SMZ-1500) and electron microscope (JEOL JSM-5800LV). The specific gravity of those glass separates from each core was also determined by the weight/volume (ASTM, 1995) method.

2.2 *Elemental analyses*

The composition of major elements in the glass shard was determined with an X-ray fluorometer (Axios PANanalytical). For this, the borate beads were made by using dry, powdered samples with Spectromelt A2 (Merck, Germany). Those beads were analyzed for major oxides by using the certified reference standard BE-N, JR-1, and JR-2 with an accuracy of (± 3 –4)%. For trace and rare earth element analyses, 0.05 g dry powdered samples were digested completely with 10 mL of an acid mixture (containing 7 : 3 HF-HNO_3); in 25 mL Savillex® screw-capped Teflon vials by following a closed digestion method. After swirling, the vials were kept on the hot plate at ~150℃ for 48 h. Following this, the contents were evaporated at 200℃ to dryness with a few drops of $HClO_4$. The residues were then dissolved in 10 mL 6.0(N) HNO_3, and the final volume was made to 250 mL with Milli-Q water. Solutions were analyzed for trace elements with HR-ICPMS (Nu Instruments Attom®, UK) by using (1 ng/mL) ^{103}Rh solution as an internal standard (Satyanarayanan et al., 2018). Certified reference materials JG-1a, JG-2, JR-2 from the Geological Survey of Japan, and G-2 from USGS, along with procedural blanks, were also analyzed by following the same protocol. Care has been

Table 1. Locations of sediment cores, water depth, core recovery, occurence depth of tephra layers, grain size distribution and specific gravity of glass shards from Toba ashes at Mahanadi offshore basin

Cores	Latitude, Longitude	Water depth/m	Core recovery/m	Depth of ash layer/mbsf	Grain size/μm				Specific gravity/ (gm·cm^{-3})
					< 2.0	2–63	63–125	> 125	
MD-19	18°59.11′N 85°41.17′E	1 480	39.08	9.64–9.72	3.31	81.13	15.6	0.0	2.7
MD-20	18°47.36′N 85°36.44′E	1866	50.08	19.14–19.19	2.01	62.44	31.29	4.26	2.6
MD-23	19°06.25′N 85°50.15′E	1 600	38.62	22.2–22.26	1.47	48.42	37.57	12.54	2.6
MD-24	19°03.48′N 85°45.59′E	1 578	31.89	18.59–18.69	1.75	62.11	30.77	5.37	2.7
MD-27	18°57.36′N 85°43.44′E	1 691	36.06	12.13–12.18	1.6	62.92	31.17	4.31	2.6

taken to eliminate isobaric interferences, which were programmed and corrected automatically. Precision and accuracy were better than 3% RSD for most of the trace and rare earth elements.

3 Results and discussion

In all the studied sediment cores, the visual observations showed about 5–10 cm thick light-colored ash layers exist at a different range of sediment depths between 9.6 mbsf to 22.2 mbsf (Table 1). Microscopic and mineralogical examinations of the coarse fractions of each ash layer indicate the considerable presence of fresh, shining, colorless volcanic glass shards along with traces of pyrites and biotites. In contrast, the finer fractions (<63 μm) showed a substantial presence of biogenic spherules resembling typical bacterial cells along with glass particles. The microscopic view of some of those mineral aggregates is presented in Fig. 3A. The physical nature and geochemical characteristics of abundant glass shards from ash layers of each core is discussed in the following section to ascertain the possible source origin of those ash layers.

3.1 *Particle size and morphology of glass shards: Qualitative assessment of volcanic ash layers*

The size, morphology, and specific gravity of glass shards from each core were studied separately, and the results are presented in Table 1. The data on particle size reveal that at all five sampling sites, the volcanic ashes were mostly dominated by silt-sized (2–63 μm) glass shards (48%-81% of the total), followed by larger sand-sized (63–125 μm) shards (16%–37%). While the abundances of relatively large (>125 μm) or very fineclay-sized (<2.0 μm) glass particles were substantially low (<10% of the total) (Table 1). It has also been noticed that the overall size distribution patterns of glass shards in ash layers considerably differ among the studied cores, but their specific gravity varies within a close range from 2.6 g/cm^3 to 2.7 g/cm^3 with an average of 2.64 g/cm^3. Furthermore, the particle-size distribution of each sample shows multimodal patterns (M_1-M_5) having characteristic sizes of 2.84 μm, 5.5 μm, 9.25 μm, 25.32 μm, and 64.95 μm (Fig. 2). The particles of medium to fine sand size were transported ~2 300 km away from the source. The shape of these shards ranges from blocky or platy to vesicular, most with a typical bubble-wall structure indicating atmospheric transport. This further suggests that the ash particles were deposited in the Mahanadi basin, bay of Bengal, directly from the atmosphere as resulting ash and were subsequently dispersed by bioturbation. Such multimodal size distribution can be attributed to tephra originating from a distal volcanic source and hence occur as poorly sorted ash aggregates (Carey and Sigurdsson, 2000; Lewis et al., 2012).

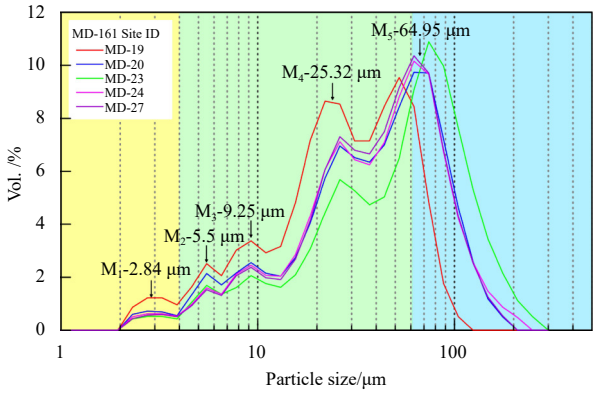

Fig. 2. Multimodal particle size distribution of volcanic tephra layers in five studied cores from Mahanadi offshore region, Bay of Bengal.

Like variable particle size, the range of color from colorless to deep brown of these glass shards also apparently indicates their compositional variability. Most of the glass shards displayed cuspate, flat, or curved platy morphology. SEM analyses showed that most of the glass shards have bubble-walled features and are characterized by smooth, slightly curved surfaces (Fig. 3B). An earlier study by Izeet (1981) indicated that usually less viscous G-type rhyolitic magma sources having temperatures more than 870℃ might develop such characteristic morphology in volcanic glass. Similar double wall morphology in Toba glass shards has also been reported in samples from other parts of the Indian Ocean (Gasparotto et al., 2000; Jumaila et al., 2017) and in the South China Sea (Rose and Chesner, 1987; Bühring and Sarnthein, 2000; Song et al., 2000).

3.2 *Major elemental composition of glass shards: Geochemical constraints on the magma source*

The major element compositions of the glass shards from the ash layers of five cores from the Mahanadi basin are dominated

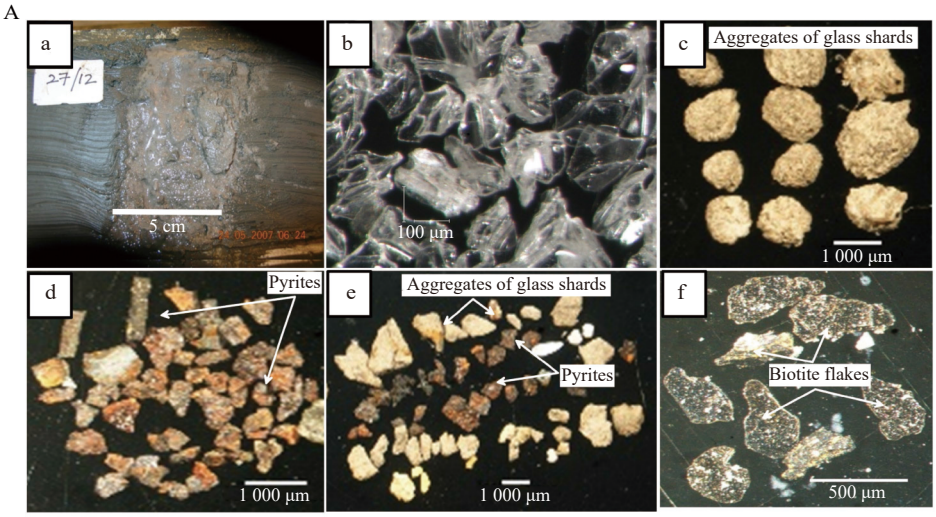

Fig. 3.

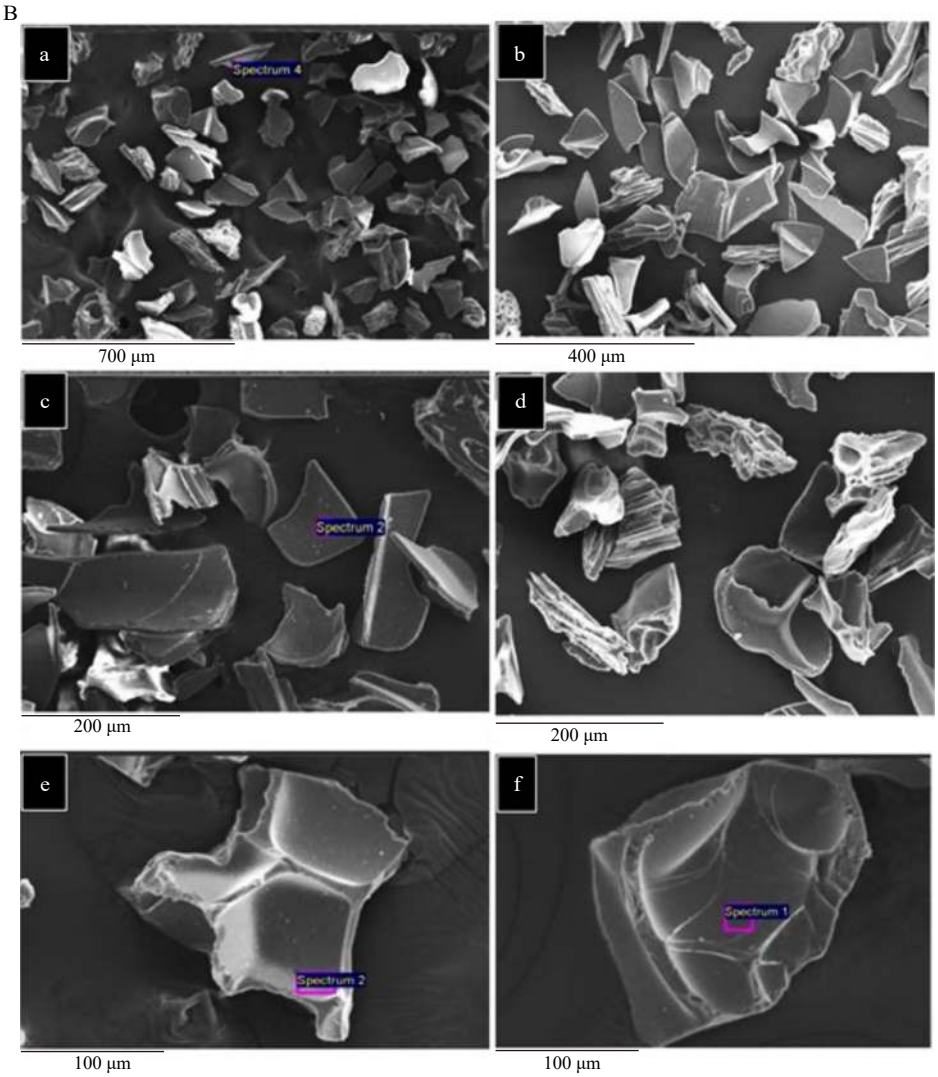

Fig. 3. A. The occurrence of volcanic ash beds in the sediment core from the Mahanadi basin (a); the microscopic image shows the occurrence of volcanic glass shards (b); the coarse fractions extract from volcanic tephra show the occurrence of aggregates of glass shards, pyrites, and biotites (c-f). B. Scanning electron micrographs of glass shards from volcanic ashes at Mahanadi basin: and glass shards of different sizes and shapes (a and b); flat and curved fragments (c); pumice shard with elongated vesicles (d); Y-shaped triple junction formed between three bubbles with smooth surface (e); Broken part of triple junction of bubble-walled glass-shard (f).

by SiO_2 (75.2%–76.2%) and Al_2O_3 (10.5%–11.3%); relative to total alkalis (i.e., Na_2O+K_2O+CaO ~8.1%–8.9%) and Fe-oxides (0.7%–1.0%)(Table 2). The elevated silic a concentrations and higher K_2O contents (>4.5%) than CaO (<0.9%) in all these glass shards match well with typical rhyolitic magma with depleted iron content and differ from andesitic volcanic sources. The plot of alkali metals against silica contents (i.e., TAS diagram) in Fig. 4A also shows the glass compositions in all five cores were

Table 2. Major element composition (wt%) of glass shards from the Mahanadi offshore region compared with the YTT from other locations. Please note that A = Central Indian Ocean Basin (Pattan et al., 1999); B = South China Sea (Song et al., 2000); C = Arabian Sea (Pattan et al., 2001); D, E, F = Glasses from YTT, MTT and OTT respectively from the Toba caldera (Chesner, 1998)

Major oxides	Cores from the Mahanadi basin					YTT from other marine environments			Glasses from the Toba caldera		
									YTT	MTT	OTT
	MD-19	MD-23	MD-24	MD-27	MD-20	A	B	C	D	E	F
SiO_2	75.98	76.20	75.64	75.22	75.74	76.81	77.48	77.06	76.8–78.2	75.2–76.9	71.9–76.4
Al_2O_3	10.86	10.48	10.69	10.92	11.26	12.77	12.42	12.44	11.9–12.9	12.6–13.9	13.3–14.4
Na_2O	2.54	2.09	2.33	2.50	3.00	3.41	2.43	3.36	2.6–2.9	2.98–3.5	3.4–3.6
K_2O	4.95	5.33	5.18	5.55	4.62	5.08	4.72	5.11	4.8–5.3	4.1–4.8	4.7–4.8
CaO	0.68	0.69	0.79	0.84	0.57	0.79	0.75	0.80	0.62–0.94	0.75–0.82	1.0–1.9
Fe_2O_3	0.80	1.15	0.95	1.09	0.77	0.92	0.85	0.88	0.84–1.2	1.2–1.4	0.6–2.5
H_2O	5.42	5.29	4.40	4.18	5.34	5.23	–	4.94	–	–	–
$Na_2O + K_2O$	7.49	7.61	7.42	7.51	8.05	–	–	–	–	–	–

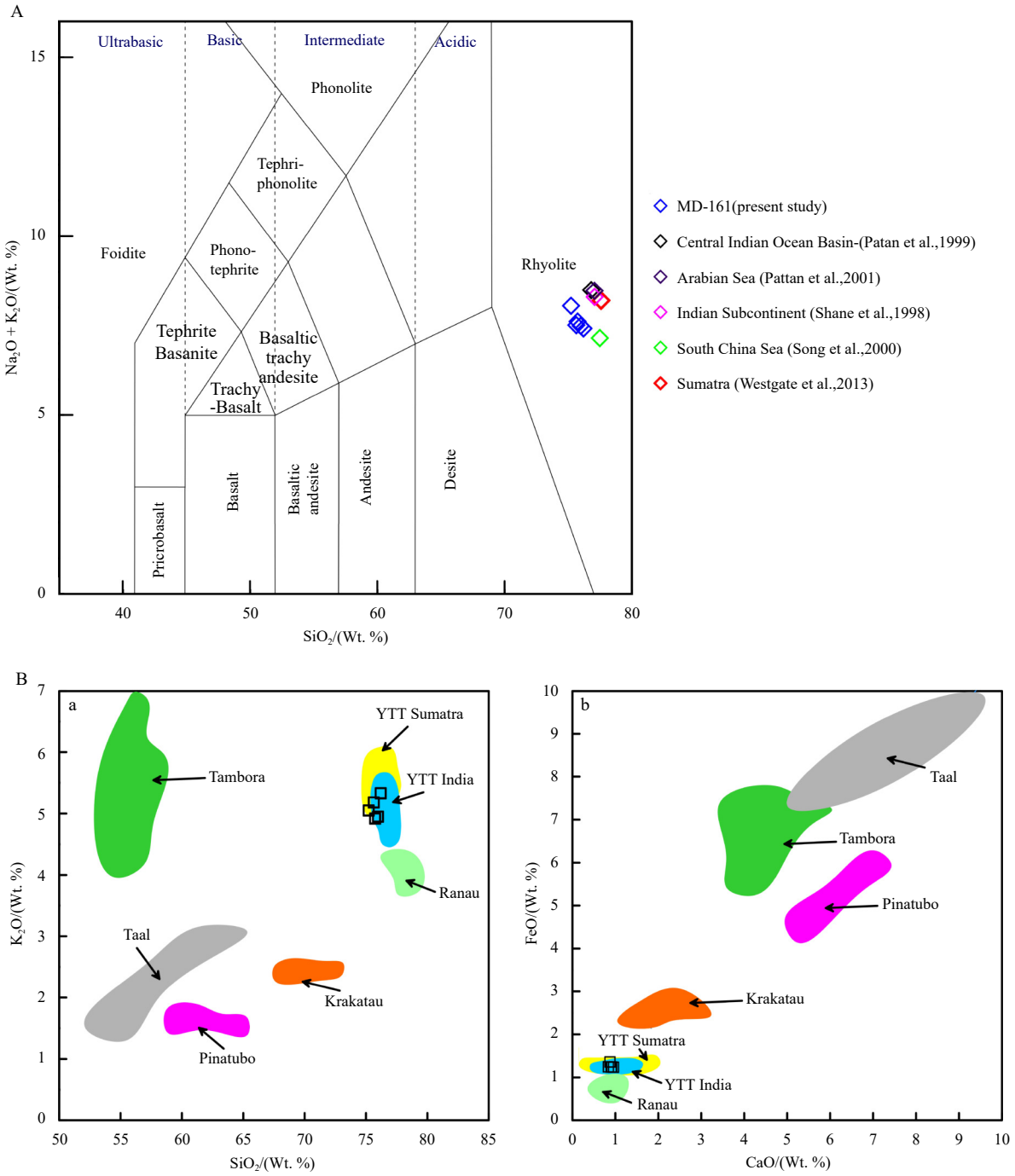

Fig. 4. A. The chemical composition of glass shards from the Mahanadi offshore, Bay of Bengal. Total alkali-silica (TAS) diagram showing the rhyolitic composition of glass shards (modified from Le Bas et al., 1986). B. Chemical correlation of glass shards from volcanic ash layer in the Mahanadi basin deposits of the YTT. The data obtained for Krakatau Volcano (Mandeville et al., 1996); Tambora Volcano (Self et al., 1984); Pinatubo, Taal, Ranau and Maninjau Volcano (De Maisonneuve et al., 2020).

very consistent, with magma having typical rhyolitic composition. Moreover, the close range of major elemental composition in glass shards from different cores further suggests all these ash deposits across the Mahanadi basin might originate from the same rhyolitic sources. In the TAS diagram, the rhyolitic glass from the Mahanadi basin closely resembles the Toba volcanic deposits reported elsewhere (Pattan et al., 2010; Srivastava and Singh, 2020; Amonkar et al., 2020). Most of the other major oxide concentrations were also found compatible with the glasses associated with Toba tuffs from other parts of the Indian Ocean, South China Sea, and as well as with volcanic glasses from the Toba caldera (Table 2).

Till date, in many parts of the Indian Ocean and adjacent continental regions, the evidence of the past three major volcanic events at Toba, Sumatra (i.e., OTT of 800 ka; MTT of 500 ka, and YTT of 74 ka) have been recorded in sedimentary columns. In most cases, the ashes that originated through those events are distinctly identified based on volcanic glass compositions (Song et al., 2000; Smith et al., 2011; Pearce et al., 2020). In the present study, the estimated concentrations of major oxides like Na_2O,

K_2O, CaO, Al_2O_3, and Fe_2O_3 in glasses from the Mahanadi basin lie close to the ranges reported in YTT from other marine environments (Table 2); but substantially differ from MTT and OTT deposits though not perceptible in the bulk composition. The comparison with proximal ash samples from Toba caldera also showed the Mahanadi basin samples also differ from the values in glasses from typical MTT and OTT deposits and resemble more YTT (Table 2). However, in contrast, the estimated values of SiO_2 (75.2%–76.2%) in present analyses were substantially less than average values in typical YTT deposits (SiO_2 > 76.5% ,Table 2), while matches well with MTT or OTT, though SiO_2 may not be the discriminating factor. Such contrasting SiO_2 contents could be the result of post-depositional alterations of glasses in marine sediment. The experimental results of Gatti et al. (2014) indicated that in aquatic environments, weathering of volcanic glasses could cause significant leaching of Si from glasses with time.

Based on the calcareous nanofossil bio-stratigraphy, Flores et al. (2014) has shown that during the late Pleistocene age, the estimated sedimentation rate was ~135 m/Ma (i.e.,13.5 cm/ka) near that site. Thus following the age-depth model based on radiocarbon dating, the ash layer at about 9.64 mbsf at the site MD-19 should correspond to the age between 70–75 ka, very similar to the YTT event. Therefore, based on major element composition and information from the age-depth model, it could ascertain the dispersion of ash from the youngest Toba events as the source for ash layers in the Mahanadi basin.

3.3 *Trace and rare earth elemental composition of glass separates: Heterogenic magma of youngest Toba event as source of volcanic ashes*

The concentrations of trace elements in volcanic glass samples from the 5 cores of the Mahanadi basin are presented in Table 3. The results show, unlike major oxides, most of those trace elements have substantial variations and apparently point toward the finer scale compositional variety among those glass samples. In particular, the lithophilic elements like Ba (187–812)×10^{-6} and Sr (31–90)×10^{-6} have a wide range of concentrations in these glass shards and were consistent with the values found in YTT deposits [Ba: (50–1 400)×10^{-6}; Sr: (0–150)×10^{-6}, Pearce et al., 2020]. The concentrations of other lithophiles, Rb (111–272)×10^{-6} and Cs (3.4–10.4)×10^{-6}(Table 3) were also substantially high, and most of them are comparable to the range of values in YTT described elsewhere [Rb = (253 ± 45)×10^{-6}; Cs = (8.3 ± 2.5)×10^{-6}; Pearce et al., 2020]. Earlier studies also showed that besides the absolute concentrations of Ba and Sr, their relative enrichment with respect to incompatible elements like Y in volcanic glasses reflects the subtle differences between the composition and evolution of magma during those Toba events (Pearce et al., 2020). It is also evident that in Figs 5a and b, the plots of Ba and Sr concentrations against Y in analyzed glass shard samples from the Mahanadi basin are compared with the data from other Toba deposits, which indicates glasses of the present study are very similar to YTT and strikingly differs from OTT or MTT deposits. In other known YTT deposits, the multiple similar clusters of Ba and Sr concentrations in volcanic glasses has referred to as diverse YTT populations with different degrees of magmatic evolution (Figs 5a and b; Westgate et al., 2013; Pearce et al., 2014, 2020). The mostly heterogeneous nature of Toba magma at the time of YTT eruption was primarily responsible for the development of such diverse YTT glass populations (Gatti et al., 2014). Thus the lower Ba/Y ratios (10.3–14.9, Table 3) in glasses from the cores MD-19, MD-23, MD-24, and MD-27 apparently belong to the intermediate cluster-III of YTT; and those differ from the higher ratio in samples from the core MD-20 (Ba = 812×10^{-6}; Ba/Y: 22.4, Table 3); representing more evolved cluster-IV (Fig. 5a). Earlier studies suggested that Toba glass shards with high Ba content corres-

Table 3. Trace element concentrations (10^{-6}) in volcanic glasses from the Mahanadi basin. The data are compared with the range of volcanic glass composition from other YTT deposits. Please note that A = YTT from India, Malaysia, Indian Ocean, Toba caldera (Srivastava and Singh, 2019 and references therein); B = YTT glass from ODP-758 site in Bay of Bengal (Jumaila et al., 2017); C = Five populations of YTT glass composition (Pearce et al., 2020); D = YTT glass shards from Central Indian Ocean Basin (CIOB) (Pattan et al., 2002)

Element concentration	YTT from the cores of Mahanadi basin					YTT from other marine environments			
	MD-19	MD-23	MD-24	MD-27	MD-20	A	B	C	D
Sc/10^{-6}	2.7510–6	1.84	2.92	1.99	2.88	1.7–3.02	4.3	–	1.54–1.93
V/10^{-6}	3.64	3.25	4.09	2.89	6.48	–	18.79	–	12.7–17.4
Cu/10^{-6}	3.05	2.14	1.65	1.54	22.5	–	19.08	–	2.43–6.2
Zn/10^{-6}	174	152	226	281	432	–	71.41	–	6.95–10.2
Ga/10^{-6}	14.4	6.84	14.2	10.4	13.9	9.01–11.08	16.55	–	8.3–12.3
Rb/10^{-6}	272	111	239	193	224	199–286	205	200–292	171–252
Sr/10^{-6}	60.3	31.0	52.4	53.5	89.9	25.8–108	87.28	28.9–113	43.7–63.8
Y/10^{-6}	41.6	18.2	36.1	31.2	36.3	28.9–64.7	29.26	36.9–69.8	22–31.7
Zr/10^{-6}	176	71.3	153	135	154	–	119	116–144	57.9–87.6
Nb/10^{-6}	18.4	7.15	16.6	15.1	15.1	10.2–22.5	8.45	17.5–23.9	11–15.8
Cs/10^{-6}	10.4	3.41	10.3	7.37	9.33	5.3–10.8	12.55	5.12–10.8	7.1–10.9
Ba/10^{-6}	453	187	537	338	812	88–1 142	527	94.5–1 191	350–514
Hf/10^{-6}	5.81	1.59	4.79	4.36	4.89	–	3.94	5.6–6.05	2.8–3.71
Ta/10^{-6}	4.07	0.91	2.99	2.37	2.22	–	1.1	2.15–3.76	1.18–1.74
Pb/10^{-6}	40.9	46.5	59.3	45.4	84.6	25.3–72.4	12.94	57.1–60.9	–
Th/10^{-6}	34.1	15.9	32.7	25.1	30.8	25.4–58	21.05	45.8–64.3	23.2–32.9
U/10^{-6}	5.73	2.50	5.92	4.34	5.01	3.99–9.97	5.82	5.28–10.5	6.6–8.1
Sr/Y	1.45	1.70	1.45	1.71	2.48	–	2.98	0.42–3.09	–
Ba/Y	10.9	10.3	14.9	10.8	22.4	–	18.01	1.36–32.7	–
Zr/Y	4.2	3.9	4.2	4.3	4.2	–	4.07	1.67–3.91	–
U/Ce	0.09	0.095	0.083	0.089	0.078	–	–	–	–

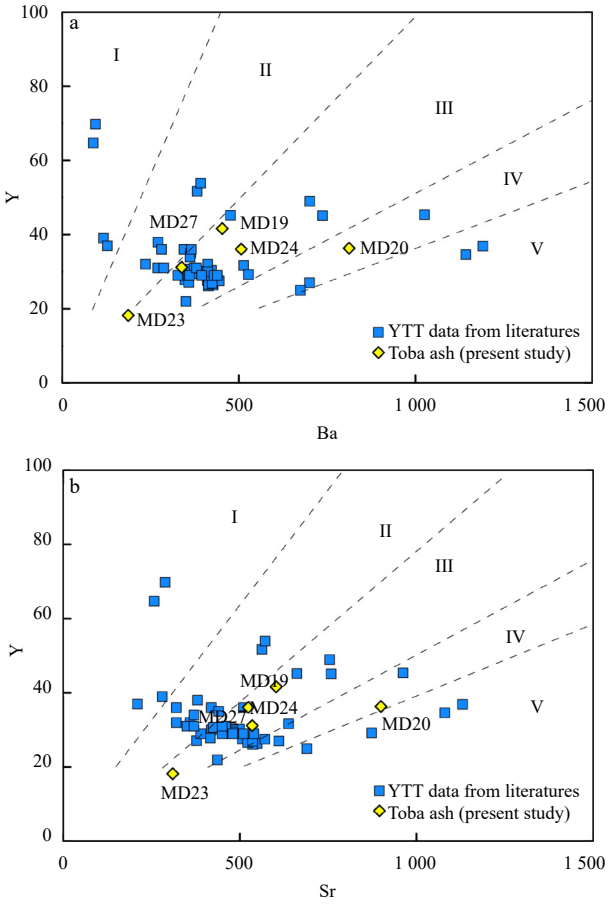

Fig. 5. The comparative plots of Ba vs. Y (a) and Sr vs. Y between volcanic glass shards from the Mahanadi basin (present study) and Toba tephra deposits in India Occan (b) (Srivastava and Singh, 2021; Pearce et al., 2020; Jumaila et al., 2017; Smith et al., 2011; Pattan, 2002; Song et al., 2000; Chesner, 1998; Westgate et al., 1998). The categorization of YTT among five different populations (I to V) was made by following Pearce et al., 2020.

pond to the magma source equilibrate at the deeper part of the magma chamber, while lower Ba values originate from late-stage emission of the larger volume of magma from shallow depths (Pearce et al., 2020). Likewise, the elevated Sr/Y ratio (= 2.48) in glasses from the southernmost core MD-20 was also similar to those reported in cluster-IV glasses of YTT (Sr/Y = 2.16 ± 0.43, Pearce et al., 2020), but the values of Sr/Y = 1.4–1.7 in other cores (Table 3) matches well with cluster-III of YTT deposits (Sr/Y = 1.57 ± 0.27; Pearce et al., 2020). The glass samples from the MD-20 cores, which originated from equilibrated magma at deeper depth, also showed higher concentration of elements (e.g., Cu, Zn, V, Pb), usually have higher mobility at elevated temperatures than those found in glasses from cores MD-19, MD-23, MD-24 and MD-27 (Table 3).

In contrast to lithophiles, the concentrations of relatively immobile high field strength elements (HFSEs) like Sc (1.8–2.9)×10^{-6}, Ga (6.8–14.4)×10^{-6}, Zr (71–176)×10^{-6}; Hf (1.6–5.8)×10^{-6}, Nb (7.1–18.4)×10^{-6}, Ta (0.9–4.1)×10^{-6}, was less in those glass samples (Table 3), but have comparable ranges reported in YTT from other marine environments (Srivastava and Singh, 2020; Pearce et al., 2020). It has also been noticed that, even at lower concentrations, these trace elements showed considerable variation among glasses from those ash layers. Studies indicate subtle variability of some HFSEs in glasses with minor overlaps representing a variety of magma compositions originating during the youngest Toba event (Pearce et al., 2020). In the present study, most of the estimated HFSEs in Mahanadi samples (except MD-23), match well with ranges (e.g. Zr = (106–169)×10^{-6}; Hf = (4.06–7.55) ×10^{-6}; Nb = (15.9–21.5) ×10^{-6}; Pearce et al., 2020) reported in more evolved magma sources (of clusters III and IV) of YTT.

The rare Earth elemental compositions of volcanic glasses from five cores of the Mahanadi basin are listed in Table 4. The total REE contents (∑REE) in these glass samples vary within the range of (61–164) ×10^{-6} with the dominance of lighter rare earth elements (LREEs > 90% of the total, Table 4). Like other immobile trace elements, the concentrations of most of the rare earth in these glass shards lie within a range very similar to those reported in other YTT deposits. Moreover, the chondrite normalized REE patterns (Fig. 6) of all glass shards had very similar trends

Table 4. REE composition (in 10^{-6}) and systematics in volcanic ash from Mahanadi basin Europium anomaly, $Eu/Eu^* = Eu_n/(Sm_n . Gd_n)^{0.5}$& Cerium anomaly, $Ce/Ce^* = 3Ce_n/(2La_n+Nd)$. Please note that A = YTT from India, Malaysia, Indian Ocean, Toba caldera (Srivastava and Singh, 2019 and references therein); B = YTT glass from ODP-758 site in Bay of Bengal (Jumaila et al., 2017); C = five populations of YTT glass composition (Pearce et al., 2020)

REEs	YTT from the cores of Mahanadi basin					YTT from other marine environments		
	MD-19	MD-23	MD-24	MD-27	MD-20	A	B	C
La	33.61	14.47	37.49	25.73	33.44	21.3–60.7	33.81	34.3–68
Ce	63.72	26.18	71.38	48.67	63.86	40.0–99.2	55.99	66–107
Pr	8.14	3.42	8.82	6.09	8.05	4.7–10.1	6.82	8.02–11.1
Nd	24.73	9.14	24.33	18.62	23.49	17.0–34.4	28.78	30.9–37.4
Sm	5.27	1.83	5.04	3.96	4.93	3.3–7.4	5.32	7.09–8.24
Eu	0.48	0.15	0.4	0.36	0.52	0.3–0.74	0.72	0.36–0.75
Gd	4.07	1.37	3.74	3	3.72	2.8–7.95	4.22	6.14–8.89
Tb	0.73	0.23	0.64	0.54	0.65	0.54–1.42	0.73	0.94–1.58
Dy	4.78	1.42	3.98	3.56	4.17	3.2–9.64	3.89	6.3–10.6
Ho	1.09	0.33	0.91	0.82	0.95	0.58–2.17	0.74	1.37–2.37
Er	3.08	0.93	2.59	2.31	2.65	1.91–6.99	2.43	4.2–7.65
Tm	0.55	0.16	0.46	0.42	0.47	0.34–1.18	0.45	0.71–1.29
Yb	4.22	1.28	3.49	3.2	3.57	2.9–7.96	3.01	4.86–8.93
Lu	0.72	0.22	0.6	0.54	0.6	0.48–1.28	0.48	0.77–1.44
∑REE	155.2	61.1	163.9	117.8	151.1	–	–	–
%LREE	90.2	92.5	92.3	90.3	91.4	–	–	–
Eu/Eu^*	0.31	0.29	0.28	0.32	0.37	–	–	–
Ce/Ce^*	0.93	0.91	0.95	0.93	0.94	–	–	–
Nd_n/Yb_n	2.10	2.57	2.51	2.09	2.37	–	–	–

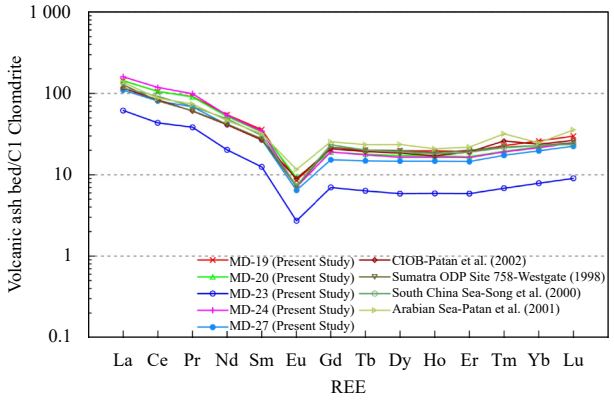

Fig. 6. Chondrite normalized REE patterns of volcanic glass shards from the Mahanadi offshore basin, Bay of Bengal are compared with those from the Indian Ocean (Westgate et al., 1998); South China Sea (Song et al., 2000); Arabian Sea (Pattan et al., 2001) and Toba caldera (Smith et al., 2011). Normalization values are obtained from Sun and McDonough (1989).

with significant LREE (La-Sm) enrichment and relatively flat HREE (Gd-Lu) profiles, might be indicative of felsic rhyolitic magma source, as mentioned before. Most of these REE-patterns (except MD161-23, which marginally differs from the rest); closely resemble the YTTs from Toba caldera and other oceanic sources. In an earlier study, it has also noticed that the relative enrichment of LREE over HREE is more prominent (Nd_n/Yb_n = 1.8–2.7, estimated with data from Pearce et al., 2020) in glass populations (PIII-PV) of YTT, originated from less voluminous deeper magma sources. Thus, in the present study, the higher REE cross-group fractionations (Nd_n/Yb_n = 2.0–2.6) in glass shards might also have a similar deep magmatic origin. All the REE patterns were characterized by very marginal negative Ce anomalies (Ce/Ce* = 0.91–0.95; Table 4) but very distinct negative Eu-anomalies (Eu/Eu* = 0.28–0.37; Table 4). The observed Eu anomaly in REE patterns of glass shards (Fig. 6) implies early crystallization of plagioclase which usually restrict Eu incorporation from the melt during magmatic evolution and thus cause depletion of Eu relative to adjacent elements (Nakamura, 1974; Westgate et al., 1998; Song et al., 2000). Belousova et al. (2006) also stated that, the changes in Eu is consistent with simple fractional crystallization during magma cooling, as the evolving liquid becomes enriched in incompatible elements and feldspar crystallization leads to enhancement of the negative Eu anomaly.

4 Conclusions

In summary, we report the occurrence of 5-10cm thick volcanic tephra layers across the offshore regions in the Mahanadi basin for the first time. The morphology, mineralogy, and chemical compositions of volcanic tephra layers recovered from this region suggest that they are mainly rhyolitic and formed from melts of the siliceous composition. The nearly comparable composition of glass shards in five cores suggests identical volcanic sources of all ash layers. Comparing the geochemical signatures of glasses to tephra composition from the Indian Ocean region indicates that these layers originated as a result of the fallout of the latest widespread Toba tephra (74 ka) from the Indonesian volcanic arc. The occurrence of fine-grained tephra also confirms a distal source and is attributed to the YTT of Sumatra, reported in the Indian Ocean region. It is further suggested that these tephra layers reported from Mahanadi offshore region can be useful and needs to be further established as a chronostratigraphic marker for regional and global quaternary correlation. Future chronological studies on this tephra layer could help in establishing a precise time-controlled stratigraphy of the Quaternary sediments from the Mahanadi basin, Bay of Bengal.

Acknowledgements

We thank the Directors of CSIR-NIO and CSIR-NGRI, for supporting this study. This work is a part of a multidisciplinary program under the aegis of the National Gas Hydrate Program (NGHP), India, on gas hydrate exploration in the Eastern continental margin of India. The incharge of IPEV operations is thanked for providing onboard technical support and facilities. This research was funded by MoES, Govt. of India. Mr. Girish Prabhu and Mr. Vijay Khedekar are thanked for XRD and SEM analyses, respectively. This is NIO contribution no. 7047.

References

Amonkar A, Iyer S D, Babu E V S S K, et al. 2020. Extending the limit of widespread dispersed Toba volcanic glass shards and identification of new *in-situ* volcanic events in the Central Indian Ocean Basin. Journal of Earth System Science, 129(1): 175, doi: 10.1007/s12040-020-01429-6

ASTM. 1995. Standard Test Method for Determination of the Point Load Strength Index of Rock. West Conshohocken, PA.

Bühring C, Sarnthein M. 2000. Toba ash layers in the South China Sea: Evidence of contrasting wind directions during eruption ca. 74 ka. Geology, 28(3): 275–278, doi: 10.1130/0091-7613(2000)28<275:TALITS>2.0.CO;2

Belousova E A, Griffin W L, O'Reilly S Y. 2006. Zircon crystal morphology, trace element signatures and Hf Isotope composition as a tool for petrogenetic modelling: Examples from eastern Australian Granitoids. Journal of Petrology, 47(2): 329–353, doi: 10.1093/petrology/egi077

Carey S, Sigurdsson H. 2000. Grain Size of Miocene volcanic layers from grain size of Miocene volcanic layers from implications for source areas and dispersal implications for source areas and dispersal. Proceedings of the Ocean Drilling Program, Scientific Results, 165: 101–113.

Chesner C A. 1998. Petrogenesis of the Toba tuffs, Sumatra, Indonesia. Journal of Petrology, 39(3): 397–438, doi: 10.1093/petroj/39.3.397

De Maisonneuve C B, Bergal‐Kuvikas, O. 2020. Timing, magnitude and geochemistry of major Southeast Asian volcanic eruptions: identifying tephrochronologic markers. Journal of Quaternary Science, 35(1-2): 272–287, doi: 10.1002/jqs.3181

Dehn J, Farrell J W, Schmincke H U. 1991. Neogene tephrochronology from Site 758 on northern Ninetyeast Ridge: Indonesian arc volcanism of the past 5 Ma. Proceedings of the Ocean Drilling Program, Scientific Results, 121: 273–295.

Fisher R V, Schmincke H U. 1984. Submarine volcaniclastic rocks. In: Fisher R V, Schmincke H U, eds. Pyroclastic Rocks. Berlin, Heidelberg: Springer. 265–296, doi: 10.1007/978-3-642-74864-6_10

Flores J A, Johnson J E, Mejía-Molina A E, et al. 2014. Sedimentation rates from calcareous nannofossil and planktonic foraminifera biostratigraphy in the Andaman Sea, northern Bay of Bengal, and eastern Arabian Sea. Marine and Petroleum Geology, 58: 425–437, doi: 10.1016/j.marpetgeo.2014.08.011

Fuloria R C, Pandey R N, Bharali B R, et al. 1992. Stratigraphy, structure and tectonics of Mahanadi offshore basin. In: Recent Geoscientific studies in the Bay of Bengal and the Andaman basin. Journal of Geological Society of India, 29: 255–265.

Gasparotto G, Spadafora E, Summa V, et al. 2000. Contribution of grain size and compositional data from the Bengal Fan sediment to the understanding of Toba volcanic event. Marine Geology, 162(2–4): 561–572, doi: 10.1016/S0025-3227(99)00090-0

Gatti E, Villa I M, Achyuthan H, et al. 2014. Geochemical variability in distal and proximal glass from the Youngest Toba Tuff eruption. Bulletin of Volcanology, 76(9): 859, doi: 10.1007/s00445-014-

0859-x

Izet G A. 1981. Volcanic ash beds: recorders of upper cenozoic silicic pyroclastic volcanism in the western United States. Journal of Geophysical Research:Solid Earth, 86(B11): 10200–10222, doi: 10.1029/JB086iB11p10200

Jumaila C P U, Pattan J N, Ahmad S M, et al. 2017. Morphology and chemical composition of ash layer of about 8Ma old from ODP-758 site, Bay of Bengal. Indian Journal of Geo-Marine Sciences, 46(5): 871–876.

Kennett J P. 1981. Marine tephrochronology. In: Emiliani C, Ed. The Oceanic Lithosphere. The Sea. New York: Wiley, 1373–1436

Lane C S, Chorn B T, Johnson T C. 2013. Ash from the Toba supereruption in Lake Malawi shows no volcanic winter in East Africa at 75 ka. Proceedings of the National Academy of Sciences of the United States of America, 110(20): 8025–8029, doi: 10.1073/pnas.1301474110

Le Bas M J, Le Maitre R W, Streckeisen A, et al. 1986. A chemical classification of volcanic rocks based on the total alkali-silica diagram. Journal of Petrology, 27(3): 745–750, doi: 10.1093/petrology/27.3.745

Lewis L, Ditchfield P, Pal J N, et al. 2012. Grain size distribution analysis of sediments containing Younger Toba tephra from Ghoghara, Middle Son valley, India. Quaternary International, 258: 180–190, doi: 10.1016/j.quaint.2011.12.002

Liang X R, Wei G J, Shao L, et al. 2001. Records of Toba eruptions in the South China Sea. Science in China Series D: Earth Sciences, 44(10): 871–878, doi: 10.1007/BF02907078

Mandeville C W, Carey S, Sigurdsson H. 1996. Magma mixing, fractional crystallization and volatile degassing during the 1883 eruption of Krakatau volcano, Indonesia. Journal of Volcanology and Geothermal Research, 74(3-4): 243–274, doi: 10.1016/S0377-0273(96)00060-1

Mascarenhas-Pereira M B L, Nath B N, Iyer S D, et al. 2016. Multiple ash layers in late Quaternary sediments from the Central Indian Basin. Journal of Volcanology and Geothermal Research, 316: 85–100, doi: 10.1016/j.jvolgeores.2016.03.011

Nakamura N. 1974. Determination of REE, Ba, Fe, Mg, Na and K in carbonaceous and ordinary chondrites. Geochimica et Cosmochimica Acta, 38(5): 754–775, doi: 10.1016/0016-7037(74)90149-5

Ninkovich D, Shackleton N J, Abdel-Monem A A, et al. 1978. K-Ar age of the late Pleistocene eruption of Toba, north Sumatra. Nature, 276(5688): 574–577, doi: 10.1038/276574a0

Pattan J N, Shane P, Banakar V K. 1999. New occurrence of Youngest Toba Tuff in abyssal sediments of the Central Indian Basin. Marine Geology, 155(3-4): 243–248, doi: 10.1016/S0025-3227(98)00160-1

Pattan J N, Shane P, Pearce N J G, et al. 2001. An occurrence of ~74 ka Youngest Toba Tephra from the Western Continental Margin of India. Current Science, 80(10): 1322–1326

Pattan J N. 2002. Volcanic ash and its enigma: a case study from the central Indian ocean basin. Journal of the Geological Society of India, 60(2): 127–130

Pattan J N, Prasad M S, Babu E V S S K. 2010. Correlation of oldest Toba tuff to sediments in the central Indian Ocean basin. Journal of Earth System Science, 119(4): 531–539, doi: 10.1007/s12040-010-0027-4

Pearce N J G, Westgate J A, Gatti E, et al 2014. Individual glass shard trace element analyses confirm that all known Toba tephra reported from India is from the *c*. 75-ka Youngest Toba eruption. Journal of Quaternary Science, 29(8): 729–734, doi: 10.1002/jqs.2741

Pearce N J G, Westgate J A, Gualda G A R, et al. 2020. Tephra glass chemistry provides storage and discharge details of five magma reservoirs which fed the 75 ka Youngest Toba Tuff eruption, northern Sumatra. Journal of Quaternary Science, 35(1-2): 256–271, doi: 10.1002/jqs.3149

Rao D G, Krishna K S, Sar D. 1997. Crustal evolution and sedimentation history of the Bay of Bengal since the Cretaceous. Journal of Geophysical Research:Solid Earth, 102(B8): 17747–17768, doi: 10.1029/96JB01339

Rose W I, Chesner C A. 1987. Dispersal of ash in the great Toba eruption, 75 ka. Geology, 15(10): 913–917, doi: 10.1130/0091-7613(1987)15<913:DOAITG>2.0.CO;2

Sastri V V, Venkatachala B S, Narayanan V. 1981. The evolution of the east coast of India. Palaeogeography, Palaeoclimatology, Palaeoecology, 36(1–2): 23–54,doi: 10.1016/0031-0182(81)90047-X

Satyanarayanan M, Balaram V, Sawant S S, et al. 2018. Rapid determination of REEs, PGEs, and other trace elements in geological and environmental materials by high resolution inductively coupled plasma mass spectrometry. Atomic Spectroscopy, 39(1): 1–15, doi: 10.46770/AS.2018.01.001

Self S, Rampino M R, Newton M S, et al. 1984. Volcanological study of the great Tambora eruption of 1815. Geology, 12(11): 659–663, doi: 10.1130/0091-7613(1984)12<659:VSOTGT>2.0.CO;2

Smith V C, Pearce N J G, Matthews N E, et al. 2011. Geochemical fingerprinting of the widespread Toba tephra using biotite compositions. Quaternary International, 246(1-2): 97–104, doi: 10.1016/j.quaint.2011.05.012

Song S R, Chen C H, Lee M Y, et al. 2000. Newly discovered eastern dispersal of the youngest Toba Tuff. Marine Geology, 167(3-4): 303–312, doi: 10.1016/S0025-3227(00)00034-7

Srivastava A K, Singh A. 2020. Lithological, physical and chemical attributes of primary volcanic ash of YTT, Purna alluvial basin, Central India. Geological Journal, 55(10): 7011–7023, doi: 10.1002/gj.3820

Srivastava A K, Singh A. 2021. Geochemistry and constrained $^{40}Ar/^{39}Ar$ dating of Youngest Toba Tuff glass shards, Purna alluvial basin, Central India. Journal of Earth System Sciences, 130: 10, doi: 10.1007/s12040-020-01513-x

Subrahmanyam V, Subrahmanyam A S, Murty G P S, et al. 2008. Morphology and tectonics of Mahanadi Basin, northeastern continental margin of India from geophysical studies. Marine Geology, 253(1-2): 63–72, doi: 10.1016/j.margeo.2008.04.007

Sun S S, McDonough W F. 1989. Chemical and isotopic systematics of oceanic basalts: implications for mantle composition and processes. Geological Society, London, Special Publicatio, 42: 313–345, doi: 10.1144/GSL.SP.1989.042.01.19

Westaway R, Mishra S, Deo S, et al. 2011. Methods for determination of the age of Pleistocene tephra, derived from eruption of Toba, in central India. Journal of Earth System Science, 120(3): 503–530, doi: 10.1007/s12040-011-0087-0

Westgate J A, Shane P A R, Pearce N J G, et al. 1998. All Toba Tephra Occurrences across Peninsular India Belong to the 75, 000 yr B. P. Eruption. Quaternary Research, 50(1): 107–112, doi: 10.1006/qres.1998.1974

Westgate J A, Pearce N J G, Perkins W T, et al. 2013. Tephrochronology of the Toba tuffs: Four primary glass populations define the 75-ka Youngest Toba Tuff, northern Sumatra, Indonesia. Journal of Quaternary Science, 28(8): 772–776, doi: 10.1002/jqs.2672